Hindawi
Geofluids
Volume 2018, Article ID 2954306, 15 pages
https://doi.org/10.1155/2018/2954306

Research Article

Sealing Behavior and Flow Mechanism of Expandable Material Slurry with High Water Content for Sealing Gas Drainage Boreholes

Guozhong Hu,[1] **Wenrui He**,[1,2] **and Changjin Lan**[1,3]

[1]*School of Mines, Key Laboratory of Deep Coal Resource Mining, Ministry of Education of China, China University of Mining and Technology, Xuzhou, China*
[2]*College of Resources and Safety Engineering, China University of Mining and Technology, Beijing, China*
[3]*Zijin Mining Group Co. Ltd., Xiamen, Fujian, China*

Correspondence should be addressed to Guozhong Hu; gzhu@cumt.edu.cn and Wenrui He; 1522331579@qq.com

Received 29 May 2018; Accepted 1 August 2018; Published 19 September 2018

Academic Editor: Wen Wang

Predrainage of coalbed gas by underground drilling is one of the main approaches for eliminating gas disasters in coal mines. Owing to the unsatisfactory sealing effect of conventional sealing materials, coalbed gas drainage boreholes face serious air leakage, resulting in a relatively low concentration of the drained gas. This study presents a new grouting solidification method for sealing boreholes using expandable materials with high water content. An experimental test method was used to study the groutability, compression resistance, and gas permeability of the expandable materials with high water content, as well as their binding properties with coal mass at different water-cement ratios. On this basis, the governing equation for slurry permeation considering the viscosity time-varying characteristics of the expandable material with high water content was established and numerically calculated. The slurry permeation patterns of the expandable material with high water content under different grouting pressures and water-cement ratios were obtained. The results show the following: (1) the expandable material with high water content was better than cement to bind with coal mass; (2) the slurry of expandable material with high water content, with a water-cement ratio above 6 : 1, is groutable, and as the water-cement ratio increases, the groutability and penetrability of the expandable material with high water content increase; (3) the optimal grouting pressure for expandable slurry with high water content is 2-3 MPa; and (4) the higher the water-cement ratio, the greater the permeation range of expandable slurry with high water content, but the increase in the permeation range is relatively small, and the optimal water-cement ratio for expandable slurry with high water content is 7 : 1. Therefore, featuring strong groutability, good sealability, high compressive strength, microexpansion, and tight binding with coal mass, expandable materials with high water content are ideal for sealing coalbed gas drainage boreholes because of their efficiency in sealing fractures in coal and rock masses around the borehole.

1. Introduction

Coalbed gas, also known as coalbed methane (CBM), is a mineral resource that coexists with coal [1]. It is not only a major cause of disasters in highly gassy mines but also a type of clean and efficient energy [2] and a strong greenhouse gas next only to CO_2 [3]. Predrainage of coalbed gas by underground drilling is one of the main approaches for eliminating gas disasters in coal mines, extracting CBM, and reducing greenhouse gas emissions from coal mines. Its basic idea is to extract coalbed gas by drilling the target coal seams in underground funnels, as shown in Figure 1. However, due to drilling and underground funnel construction as well as stress disturbances in gas drainage, there are numerous fractures in coal and rock masses around a gas drainage borehole [4] and these fractures are in a state of dynamic change, which makes it difficult to seal the gas drainage boreholes, which face severe air leakage, resulting in a low gas concentration [5]. For

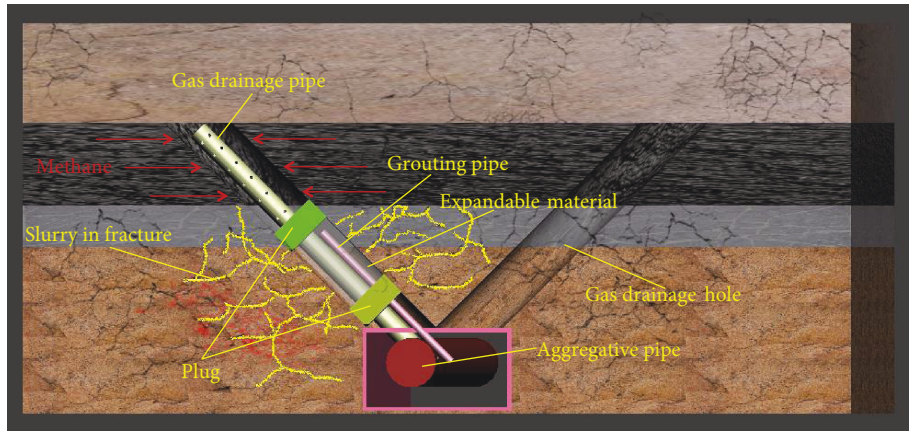

Figure 1: Schematic of sealing gas drainage boreholes using expandable material with high water content.

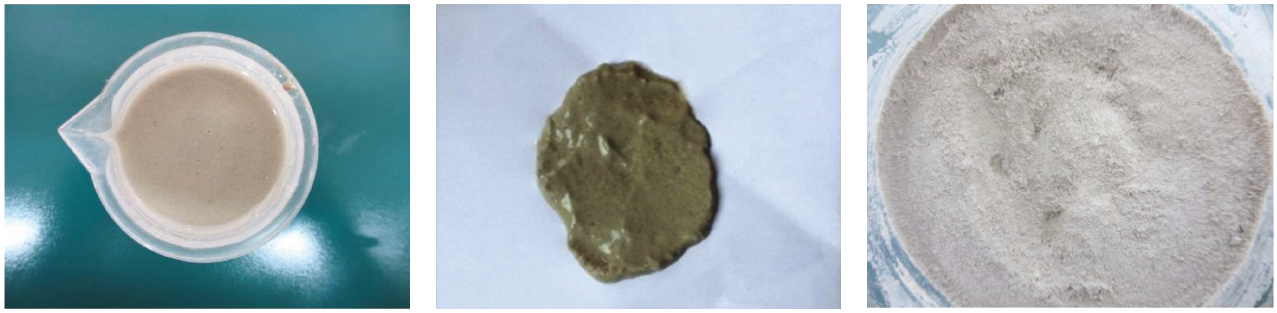

(a) (b) (c)

Figure 2: Variation of expandable material with high water content over time: (a) slurry state, (b) cementitious state, and (c) solidified state.

example, the concentration of gas predrained at approximately 65% of the stope faces of coal mines in China is below 30% [6], which severely limits the large-scale exploitation of coalbed gas [7–10].

Traditional sealing materials mainly consist of cement mortar and polyurethane material. The cement mortar is prone to shrink and fracture, and ordinary cement particles are too big to enter the microfractures of the coal mass [11], whereas polyurethane softens and shrinks in the presence of water. Moreover, with poor permeability, it is difficult for polyurethane to infiltrate into the fractures of coal and rock masses around the borehole [12]. Polyurethane thus cannot effectively improve the strength of coal mass around the borehole or prevent the formation and expansion of fractures in coal and rock masses around the borehole, resulting in a relatively low concentration of gas drainage. How to effectively seal the fractures in coal and rock masses around the borehole, increase the strength of coal and rock masses around the borehole, and maintain coal and rock masses around the borehole in a long-term, low-permeability state has become a common scientific and technological problem of great concern in the field of coal mine security worldwide [13–15].

To solve the problem of difficulty in sealing fractures in coal and rock masses around the borehole [16–20], a new grouting solidification method is proposed in this study to seal fractures in coal and rock masses around the boreholes using an expandable material with high water content (as shown in Figure 1). The expandable material with high water content used in this method is a novel material formed by adding expander to high water content material [21]. The material is characterized by good fluidity, and the slurry induration features slight expansion, strong plasticity, and rapid solidification; it is greatly applicable for the sealing of gas drainage boreholes. Hence, to investigate the sealability of this material, the groutability, compression resistance, and sealability of the expandable material with high water content were explored in this study and the permeation pattern of expandable slurry with high water content in the fractures in coal and rock masses surrounding the borehole was analyzed.

2. Expandable Material with High Water Content

With high water content, the expandable material was composed of material A, material B, set-retarding dispersant AA, and quick-setting agent BB [22]. The solidification process of the expandable material with high water content is shown in Figure 2. Added as an auxiliary material to the material with high water content, material C made the slurry with high water content expand during the solidification process, so that it could better bind with the coal mass to

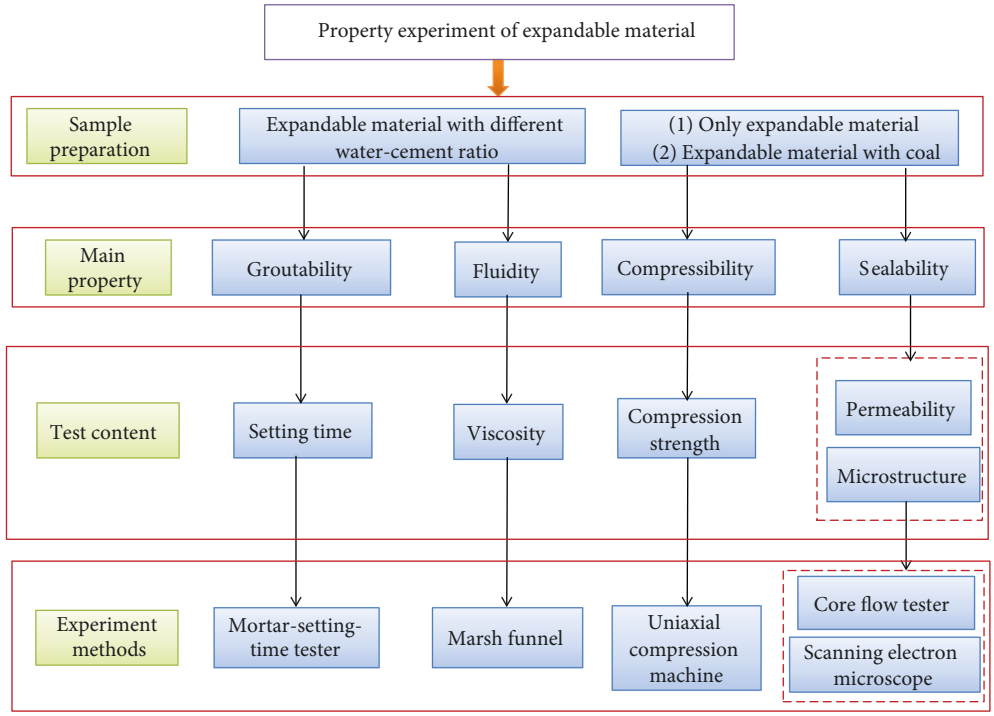

Figure 3: Experimental procedures to study the properties of the expandable material with high water content.

enhance the material's performance in sealing fractures in coal and rock masses around coalbed gas drainage boreholes.

Material A in the material with high water content was independently refined from bauxite and gypsum, and material B was mixed by gypsum and lime. During the preparation of the expandable slurry with high water content, materials A and B were used in a ratio of 1 : 1, AA was added to material A, and BB was added to material B. The slurry made of material A alone and that made of material B alone were ordinary Newtonian fluids that did not solidify until 30–40 h later. However, the slurry formed by mixing materials A and B was a non-Newtonian fluid that quickly hydrated and solidified.

3. Sealing Behavior of Expandable Material Slurry with High Water Content for Sealing Gas Drainage Boreholes

Figure 3 shows the experimental procedures followed to study the groutability, compressive strength, and sealability of the expandable material with high water content.

3.1. Methods

3.1.1. Groutability

(1) Setting Time. The setting time of the slurry or solution includes the initial setting time and the final setting time [23]. The initial setting time refers to the time from the moment when the material is mixed with water to the moment when the slurry or solution begins to lose its plasticity. The final setting time refers to the time from the moment when the material is mixed with water to the moment when the slurry or solution loses its plasticity completely. In this study, four expandable slurries with high water content were prepared, with the water-cement ratios being 4 : 1, 5 : 1, 6 : 1, and 7 : 1, and stirred for 5 min. A mortar-setting-time tester was used to measure the pressure values of the expandable slurries with high water content over time, and the pressure values obtained were substituted into the following equation to calculate the penetration resistance of the slurries over time [24]:

$$f_p = \frac{N_p}{A_p}, \tag{1}$$

where f_p denotes the penetration resistance (in MPa), which is precise to 0.01 MPa, N_p is the static pressure (in N) when the penetration depth reaches 25 mm, and A_p is the cross-sectional area of the penetration test needle, which is 30 mm^2.

The phasic change in the solidification rate of the slurry can be represented by the slope of the time-penetration resistance curves. The time-penetration resistance curve of the slurry was plotted, and the setting time of the slurry was determined by the cutoff point of the slope change of the curve.

(2) Fluidity. Viscosity is an important index with which to measure the fluidity of the slurry [24]. The expandable slurry with high water content with ideal fluidity can fully fill fractures in coal and rock masses around the gas drainage borehole and expand the grouting range, thereby improving the gas drainage outcome. Therefore, the fluidity of the slurry can be reflected by measuring its viscosity.

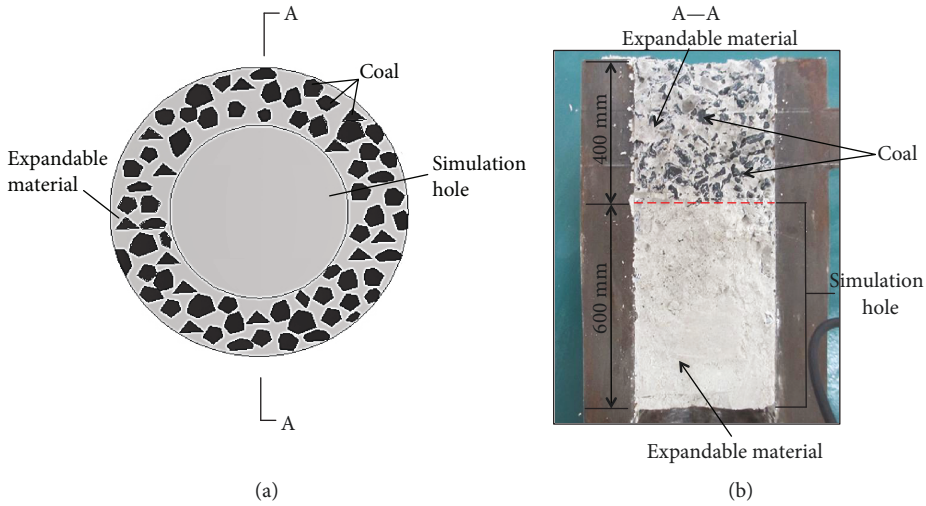

Figure 4: Model of induration of expandable material with high water content consolidated with coal masses: (a) schematic of borehole sealed by slurry and (b) model profile.

First, the effects of water-cement ratio, set-retarding dispersant AA, quick-setting agent BB, and expander C in the expandable material with high water content on the viscosity of the slurry were studied separately. Four expandable slurries with high water content were prepared at the mass ratios listed below and stirred for 5 min. A fluidity test was carried out on the above-prepared expandable slurries with high water content using the Marsh funnel [25]. The mass ratios of the four different slurries were the following: (1) A : B : AA : BB : C = 5 : 5 : 3 : 2 : 2, and the water-cement ratio being W : 1 (W = 20, 16, 13, 11, 9, 8, 7, 6, 5, 4, and 3); (2) A : B : AA : BB : C : water = 5 : 5 : x : 2 : 2 : 75, (x = 1–7); (3) A : B : AA : BB : C : water = 5 : 5 : 3 : y : 2 : 75, (y = 1–7); (4) A: B : AA : BB : C : water = 5 : 5 : 3 : 2 : h: 75, (h = 1–7).

3.1.2. Compressive Strength. After the material is grouted into the gas drainage borehole and factures in coal and rock masses around the borehole and becomes solidified, the compressive strength of the expandable slurry with high water content will affect the stability of the gas drainage borehole and its surrounding coal and rock masses, as well as the number of regenerated fractures, thereby influencing the gas drainage outcome. Hence, two samples were prepared in this study, that is, the compressed induration of the expandable material with high water content and the compressed induration after grouting the expandable material with high water content prepared according to the distribution characteristics of the slurry in the borehole and coal mass into the broken coal mass (as shown in Figure 4). These samples were used to investigate the influence pattern of different water-cement ratios on the induration of expandable material with high water content, as well as the induration of expandable material with high water content and coal mass.

The sample production is as follows: Firstly, the expandable slurries with high water content, with the water-cement ratios being 7 : 1, 8 : 1, and 9 : 1, were stirred for 5 min. The mass ratio of each component in these slurries was A : B : AA : BB : C = 5 : 5 : 3 : 3 : 3. Secondly, the slurries were injected into the mold to make two groups of specimens. The first specimen was the solidified expandable material with high water content with a height of 100 mm and a diameter of 50 mm (as shown in Figure 4(b)). The height of the second specimen was 60 mm, representing the solidified slurry in the borehole. An induration of broken coal masses bound with expandable material with high water content was 40 mm high, with a diameter of 50 mm, representing the strength of the induration after the slurry was injected into the borehole (as shown in Figure 5(b)). The specimens were then placed in a curing box for 10 d before being used in the uniaxial compression test.

3.1.3. Sealability

(1) Permeability. By measuring the permeability of the expandable material with high water content, we can determine its sealability after sealing fractures around the borehole. In this test, a core flow tester was used to measure the permeability of the expandable materials with high water content whose water-cement ratios were 6 : 1, 7 : 1, and 8 : 1. The specimens were 100 mm high and 50 mm in diameter.

(2) Microstructure. From the microstructure of the induration of expandable material with high water content and coal mass, we observed the structural composition and fracture filling of the induration of expandable material with high water content and coal mass and obtained the permeability of expandable slurry with high water content in fractures in coal and rock masses around the gas drainage borehole, as well as the binding between the expandable slurry with high water content and coal and rock masses. The experimental method is as follows: (1) A plastic tube with a diameter of 75 mm was inserted into the center of a plastic bucket with a diameter of 300 mm; the wet coal powder was poured into the gap between the plastic bucket and the plastic tube and then pressed. After ensuring that the coal mass was dense

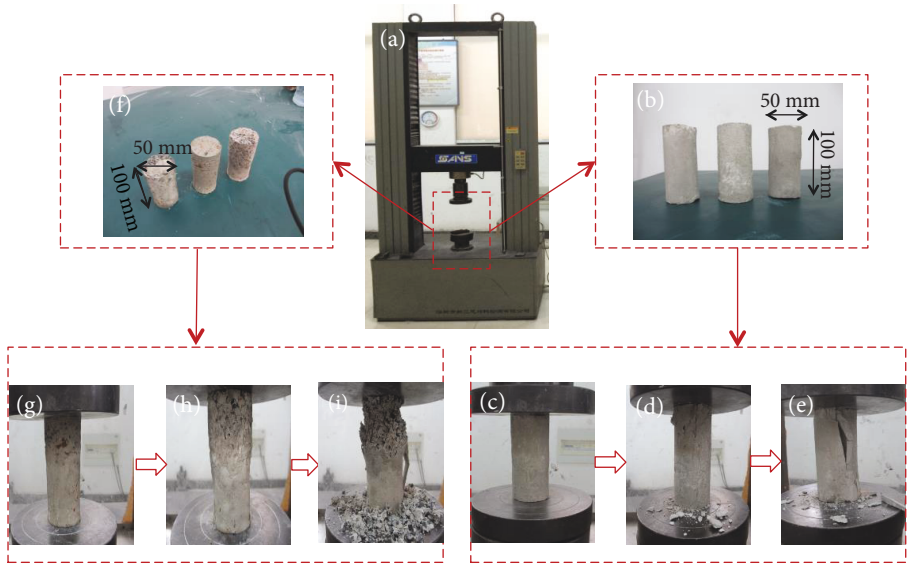

Figure 5: Compression test of induration of expandable material with high water content and induration of expandable material with high water content consolidated with coal masses: (a) uniaxial compression tester, (b) induration specimen of expandable material with high water content, (c–e) compression tests of expandable material with high water content, (f) induration specimen of expandable material with high water content consolidated with coal masses, and (g–i) compression test of induration of expandable material with high water content consolidated with coal masses.

and the plastic bucket was filled with coal powder, the plastic tube was rotated several times and then taken out to make the simulated borehole. Two simulation models were completed successively in this way; (2) The mixed cement slurry was injected into the first simulated borehole and the mixed expandable slurry with high water content was injected into the second simulated borehole; (3) The two grouted experimental models were cured in the same environment for 5 d. After the slurries in the boreholes of both models were solidified, the coal powder that had not been permeated and solidified by the slurries was slowly peeled from the outside to the inside to observe the permeation of the slurries in coal masses surrounding the boreholes; and (4) The two models were split radially and a scanning electron microscope (Quanta 250, FEI Manufacturer, USA) was applied to observe the permeation and binding of the two slurry indurations with the walls of the boreholes.

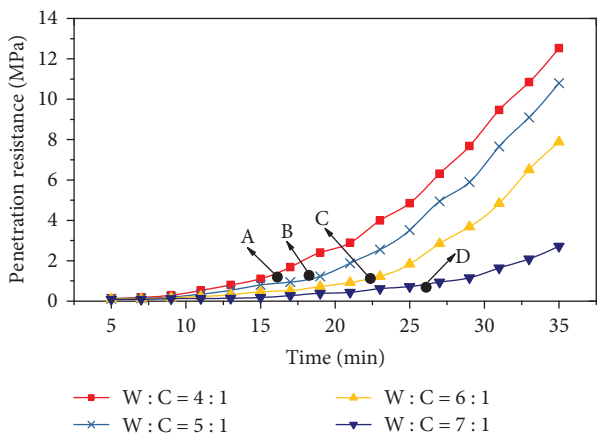

Figure 6: Initial setting time-penetration resistance.

3.2. Results and Discussion

3.2.1. Penetration Resistance. Figure 6 shows the time-penetration resistance curves of expandable slurry with high water content at different water-cement ratios. Before the cutoff point at which the time-penetration resistance curves show any phasic change, each curve's growth rate over time is slow with a small increase, whereas after the cutoff point of each curve, the growth rate accelerates with a rapidly expanding increase, namely, the solidification rate of the slurry changes from a stage featuring slow growth to one characterized by rapid growth. Therefore, according to characteristics of the curves in Figure 3, we can intuitively determine points A, B, C, and D, which are the cutoff points dividing the phasic changes of the penetration resistance of expandable slurry with high water content at different water-cement ratios over time, that is, the initial setting times of expandable materials with high water content at water-cement ratios of 4 : 1, 5 : 1, 6 : 1, and 7 : 1 are 15.5, 19, 23, and 25.5 min, respectively.

Figure 7 shows the relationship between the final setting time and penetration resistance of expandable slurry with high water content. The penetration resistance of expandable slurry with high water content increases with time until it reaches its maximum value. However, the growth rate of the time-penetration resistance curves begins to decrease after reaching the maximum, that is, the solidification rate of the slurry reaches a maximum value during a rapid growth phase, and then enters a slow growth phase until it completely

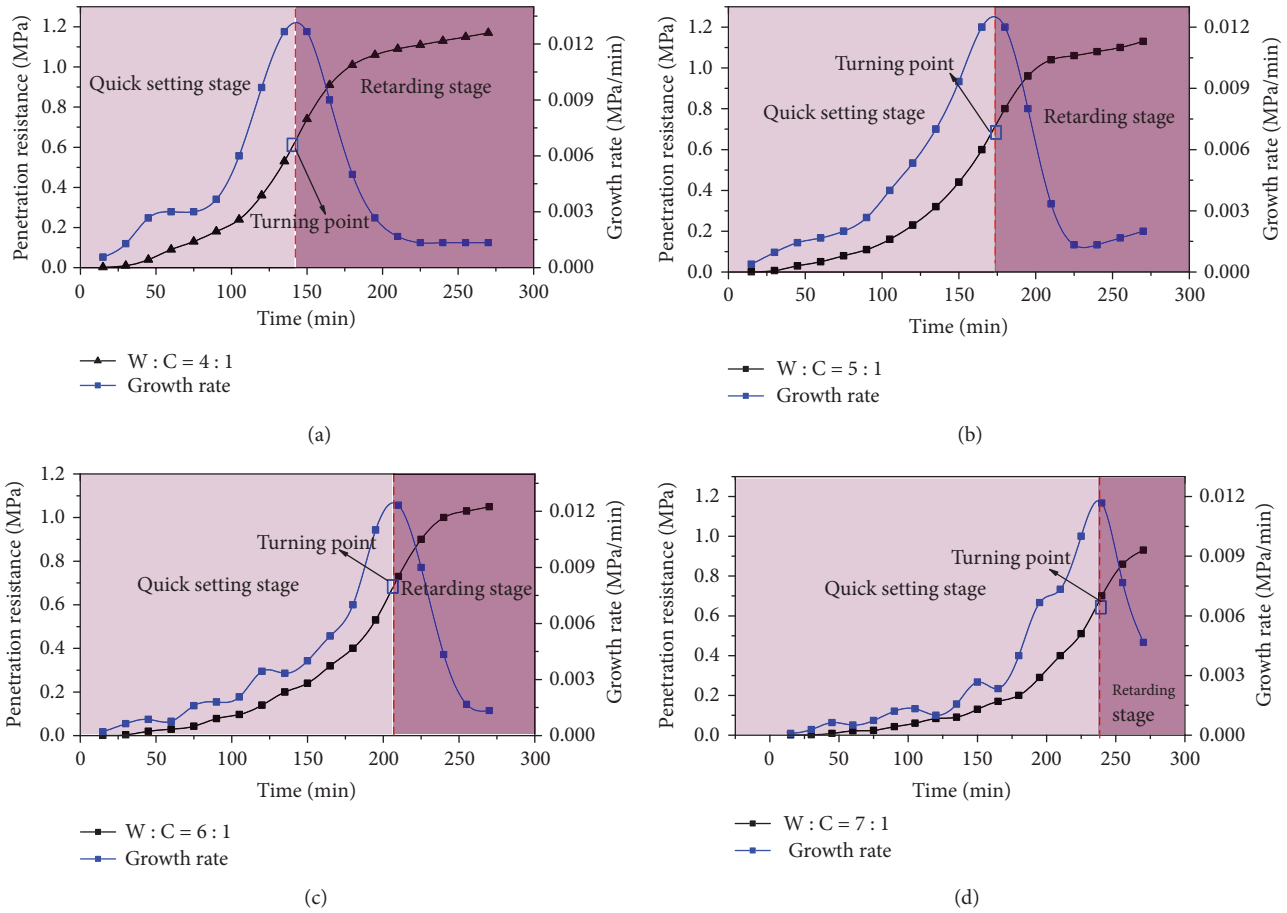

Figure 7: Relationship between the final setting time and penetration resistance of expandable slurry with high water content.

solidifies. Therefore, the time corresponding to the points at which the growth rates of the time-penetration resistance curves reach their maximum values was taken as the final setting time. Points E, F, G, and H in the figure are the cutoff points dividing the phasic changes of the penetration resistance of expandable slurries with high water content over time, which is the final setting time of expandable slurries with high water content at different water-cement ratios. As shown in the figure, the final setting times of expandable materials with high water content at water-cement ratios of 4 : 1, 5 : 1, 6 : 1, and 7 : 1 are 148, 172, 205, and 245 min, respectively.

3.2.2. Fluidity. Figure 8 shows the relationship between the water-cement ratio and funnel viscosity of expandable material with high water content. By testing the fluidity of expandable slurries with high water content, the funnel viscosity of expandable slurries with high water content at different water-cement ratios was obtained. The funnel viscosity of expandable slurries with high water content increases with increasing water-cement ratio; when the water-cement ratio is 20 : 1, the funnel viscosity is 11 s, and when the water-cement ratio is 16 : 1, the funnel viscosity is 12 s. After that, the funnel viscosity slowly increases with decreasing water-cement ratio; when the water-cement ratio is 7 : 1, the funnel viscosity rapidly increases to 42 s, and a significantly increased growth rate is observed. When the water-cement ratio is 6 : 1, the funnel viscosity reaches 50 s, and the slurry can flow slowly, and when the water-cement ratio is 3 : 1, the funnel viscosity can reach 145 s, and, with the flow rate slowing significantly, it is difficult for the slurry to flow.

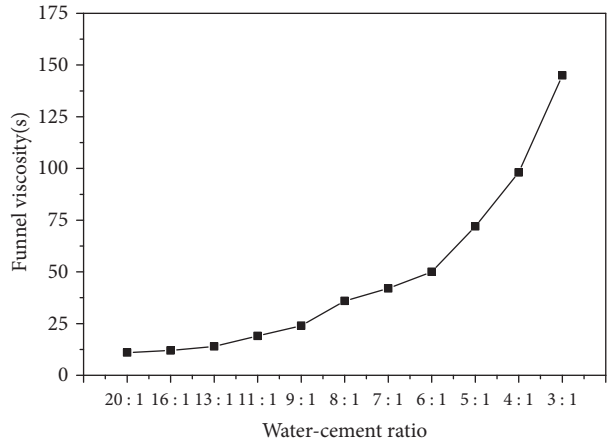

Figure 8: Relationship between water-cement ratio and funnel viscosity of expandable material with high water content.

As shown in Table 1, with an increasing amount of material AA, the funnel viscosity of the expandable slurry with

Table 1: Influences of materials AA, BB, and C on the funnel viscosity of expandable slurries with high water content.

Experimental number	Material AA		Material BB		Material C	
	Reagent proportion (%)	Funnel viscosity (s)	Reagent proportion (%)	Funnel viscosity (s)	Reagent proportion (%)	Funnel viscosity (s)
Group 1	1	14	1	15	1	15
Group 2	2	15	2	15	2	16
Group 3	3	14	3	16	3	16
Group 4	4	15	4	18	4	17
Group 5	5	16	5	19	5	19
Group 6	6	16	6	22	6	22
Group 7	7	17	7	25	7	23

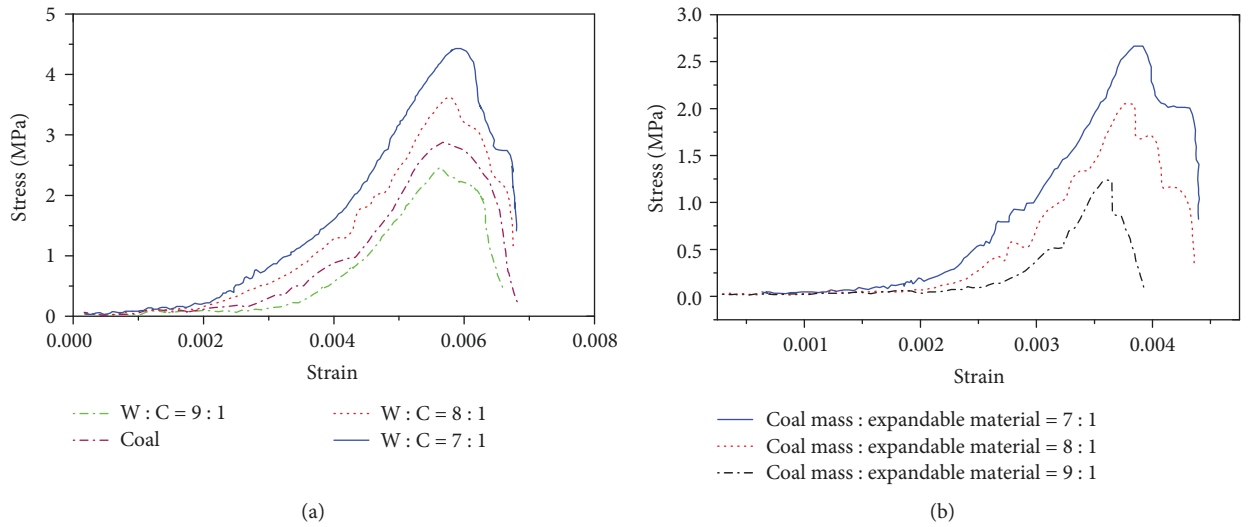

Figure 9: Stress-strain curves: (a) compression curves of expandable materials with high water content of different water-cement ratios (W : C) and (b) consolidated with coal masses of different coal-slurry ratios.

high water content changes slightly, and when the set-retarding dispersant increases from 1% to 7%, the funnel viscosity only increases by 3 s. Therefore, material AA has little effect on the viscosity of the expandable slurry with high water content. Moreover, as the amounts of materials BB and C increase, the funnel viscosity of the expandable slurry with high water content also increases constantly. As the amounts of materials BB and C increase from 1% to 7%, the funnel viscosity of the slurry increases by 10 and 8 s, respectively. Hence, materials BB and C have a great influence on the viscosity of the expandable slurry with high water content.

3.2.3. Compressive Strength. Figure 9(a) shows the stress-strain curves of the induration specimens and pure coal specimens of expandable slurries with high water content at water-cement ratios of 9 : 1, 8 : 1, and 7 : 1, respectively. It can be seen from the figure that the slopes of the curves of the induration specimens of expandable slurries with high water content at water-cement ratios of 9 : 1, 8 : 1, and 7 : 1 range from small to large successively before the peak, indicating that as the water-cement ratio decreases, the elasticity modulus of the induration specimen of expandable slurries with high water content increases, along with its ability to resist deformation. The peaks of curves 1, 2, and 3 increase in turn, indicating that with the decrease of the water-cement ratio, the strength of the induration specimen of expandable slurries with high water content rises. The maximum strengths of expandable slurries with high water content at water-cement ratios of 9 : 1, 8 : 1, and 7 : 1 are 2.15, 3.42, and 4.26 MPa, respectively. The postpeak stresses of curves 1, 2, and 3 drop more rapidly, which implies that as the water-cement ratio decreases the plasticity of the induration of expandable slurries with high water content gradually decreasing, whereas its brittleness increases.

The elastic modulus (resistance to deformation) of the pure coal specimen is located between the indurations of expandable slurries with high water content at water-cement ratios of 9 : 1 and 8 : 1; the maximum strength of the pure coal specimen is located between the two, the value of which is 3.05 MPa. In addition, as indicated by the postpeak slope of the curve, the degree of destruction of the pure coal specimen is also between the two. It can also be seen from the figure that when the water-cement ratio of expandable

Table 2: Permeability of expandable slurries with high water content sample under confining pressure 3.0 MPa.

W : C	6 : 1	7 : 1	8 : 1
Permeability (mD)	3.85	4.32	5.26

slurry with high water content is less than 8 : 1, the elastic modulus and uniaxial compression resistance of its induration are greater than those of coal masses.

Figure 9(b) shows the stress-strain curves of expandable slurries with high water content consolidated with coal masses when the mass ratios of coal and expandable slurries with high water content are 9 : 1, 8 : 1, and 7 : 1, respectively. As shown in the figure, the slopes of the curves of expandable slurries with high water content consolidated with coal masses at mass ratios of 9 : 1, 8 : 1, and 7 : 1 ranging from small to large successively before the peak, indicating that the higher the mass of expandable slurries with high water content grouted into the coal masses, the larger the elasticity modulus of the induration specimen of slurries consolidated with coal masses, and the stronger the resistance to deformation, with the maximum strengths of the compression failure being 2.75, 2.23, and 1.28 MPa, respectively. The post-peak stresses of curves of expandable slurries with high water content consolidated with coal masses at mass ratios of 9 : 1, 8 : 1, and 7 : 1 drop at a lower rate, indicating that as more slurry is injected in the induration specimen of slurries consolidated with coal masses, the plasticity of the induration specimen of slurries consolidated with coal masses gradually decreases, whereas its brittleness increases.

3.2.4. Gas Permeability. The permeabilities of the induration specimens of expandable slurries with high water content at water-cement ratios of 8 : 1, 7 : 1, and 6 : 1 were tested and measured at a confining pressure of 3.0 MPa, the results of which are shown in Table 2.

As shown in Table 2, the permeabilities of the induration specimens of expandable slurries with high water content increase as the water-cement ratio rises. The permeability is divided into five grades: (1) a permeability greater than 1000 mD indicates excellent permeability; (2) a permeability of 100–1000 mD denotes good permeability; (3) a permeability of 310–100 mD indicates medium permeability; (4) a permeability of 1–10 mD indicates weak permeability; and (5) a permeability of less than 1 mD denotes ultralow permeability. Since the permeability of expandable material with high water content is in the range 1–10 mD, the induration specimen of expandable material with high water content is characterized by weak permeability, indicating that the expandable material with high water content has poor gas permeability and thereby possesses an ideal sealing effect.

3.2.5. Adhesiveness of the Expandable Material with High Water Content. Figure 10(a) shows the microstructure of the expandable material with high water content at a magnification scale of 80 times, in which relatively clear textures can be found at the boundary where the cement is incorporated with the wall of coal masses. However, in Figures 10(a), the expandable material with high water content is fully integrated with the wall of coal masses and the boundary between the two is blurred. As shown in Figure 10(b), where the microstructure is magnified 2000 times, the gap between the cement and the wall of coal masses is comparatively obvious, whereas the expandable material with high water content binds better with the wall of coal masses, and the gap between them is smaller than that between the cement and the wall of coal masses. Taken together, the expandable material with high water content has better adhesion than the cement in the process of bonding with the wall of coal masses.

4. Flow Mechanism of the Expandable Material Slurry with High Water Content in Coal and Rock Mass Fractures

4.1. Governing Equation

(1) Viscosity time-varying function is as follows.

The kinematic viscosities of expandable slurries with high water content at water-cement ratios of 6 : 1, 7 : 1, and 8 : 1 were obtained. The following viscosity equation was gained by fitting the data curve

$$\mu_1(t) = 4.00 \times 10^{-5} t^6 - 1.10 \times 10^{-3} t^5 + 1.14 \times 10^{-2} t^4 - 4.96 \times 10^{-2} t^3 + 7.96 \times 10^{-2} t^2 - 1.83 \times 10^{-2} t + 0.35, \quad (2)$$

$$\mu_2(t) = 6.00 \times 10^{-5} t^6 - 2.00 \times 10^{-3} t^5 + 2.24 \times 10^{-2} t^4 - 0.11 t^3 + 0.24 \times t^2 - 0.12 t + 0.17, \quad (3)$$

$$\mu_3(t) = 5.00 \times 10^{-5} t^6 - 1.60 \times 10^{-3} t^5 + 1.85 \times 10^{-2} t^4 - 9.58 \times 10^{-2} t^3 + 0.212 t^2 - 0.113 t + 0.12, \quad (4)$$

where t denotes time (min) and $\mu_1(t)$, $\mu_2(t)$, and $\mu_3(t)$ (in Pa · s) represent the time-varying viscosities of the expandable material with high water content at water-cement ratios of 6 : 1, 7 : 1, and 8 : 1, respectively.

(2) Porosity of coal and rock mass is as follows [26].

$$\phi = 1 - \frac{1 - \phi_0}{1 + \varepsilon_v} \left(1 - \frac{p - p_0}{K_s}\right). \quad (5)$$

Here, ϕ denotes the porosity, ϕ_0 is the initial porosity, ε_v the volumetric strain of the coal and rock masses, p (in Pa) is the pressure of the fluid, p_0 (in Pa) is initial pressure of the fluid, and K_S represents the volumetric compression modulus of the coal and rock masses.

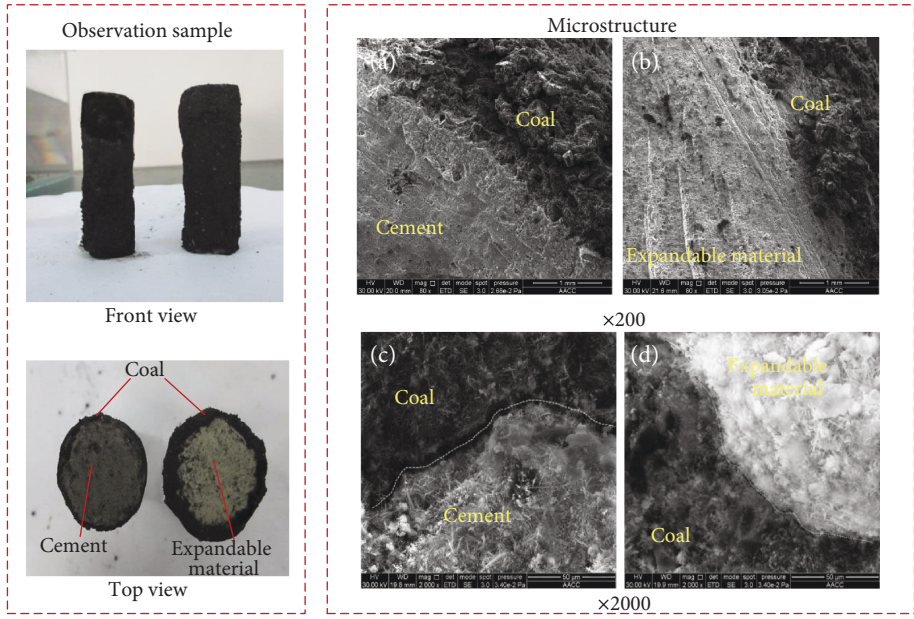

FIGURE 10: Microstructure observation of coal masses bound with cement and expandable material with high water content: (a, b) 200x magnification and (c, d) 2000x magnification.

(3) Permeability under isothermal conditions was obtained per the Kozeny-Caman equation in permeation fluid mechanics.

$$k = \frac{k_0}{1+\varepsilon_v}\left[p + \frac{\varepsilon_v}{\phi_0} + \frac{(p-p_0)(1-\phi_0)}{K_s\phi_0}\right]. \quad (6)$$

Here, k denotes the permeability and k_0 is the initial permeability.

(4) Flow equation of the slurry is as follows [27].

$$-\nabla\left(\frac{k}{\mu(t)}\nabla p\right) + \frac{\partial\varepsilon_v}{\partial t} + \left(\frac{(1-\phi)}{K_s} + \frac{\phi}{K_f}\right)\frac{\partial p}{\partial t} = 0. \quad (7)$$

Here, K_f is the volumetric compression modulus of the fluid, μ (in Pa · s) is the kinematic viscosity of the fluid, and g (in kg/s^2) is the gravitational acceleration.

(5) Reflecting the solid-liquid stress coupling, the effective stress field equation is as follows.

$$\sigma_{ij} = 2G\varepsilon_{ij} + \lambda\delta_{ij} - \phi\delta_{ij}p. \quad (8)$$

Here, σ_{ij} is the stress tensor, λ and G are the Lamé constants, where $\lambda = Ev/(2(1+v)(1-v))$ and $G = E/2(1+v)$, and δ_{ij} is the Kronecker delta.

(6) The stress field control equation of the coal and rock masses is as follows.

$$Gu_{i,jj} + \frac{G}{1-2v}u_{j,ij} + \phi p_i + F_v = 0. \quad (9)$$

Here, $u_{j,jj}$ and $u_{i,jj}$ denote the displacement tensors and F_v (N/m^3) is the volume force.

4.2. Calculation Principle and Assumptions

4.2.1. Calculation Principle. The schematic of the numerical analysis is shown in Figure 11, where the pressure of the slurry affects the volumetric strain of coal and rock masses, thereby affecting the porosity and permeability, while the change of the porosity and permeability will affect the permeability diffusion pressure of the slurry in the coal masses. As an important parameter, the viscosity of the slurry has a great influence on permeability and diffusion of the slurry. In this study, we focus on analyzing the impact of the time-varying characteristics of the viscosity of the expandable material with high water content on the permeability pressure and the diffusion range of the slurry.

4.2.2. Assumptions. In this study, the following assumptions were made regarding the model proposed to calculate permeability and diffusion of the slurry in the stratum with fractures caused by gas drainage boreholes: (1) the strata are homogeneous isotropic porous media, (2) the upper and lower borders of all the strata are impermeable, (3) the effect of gravity on permeability and diffusion of the slurry is ignored, and (4) the parameters of the injected media are selected according to the actual stratigraphic investigation and laboratory test results, and the grouted strata satisfy the conditions for grouting on the whole.

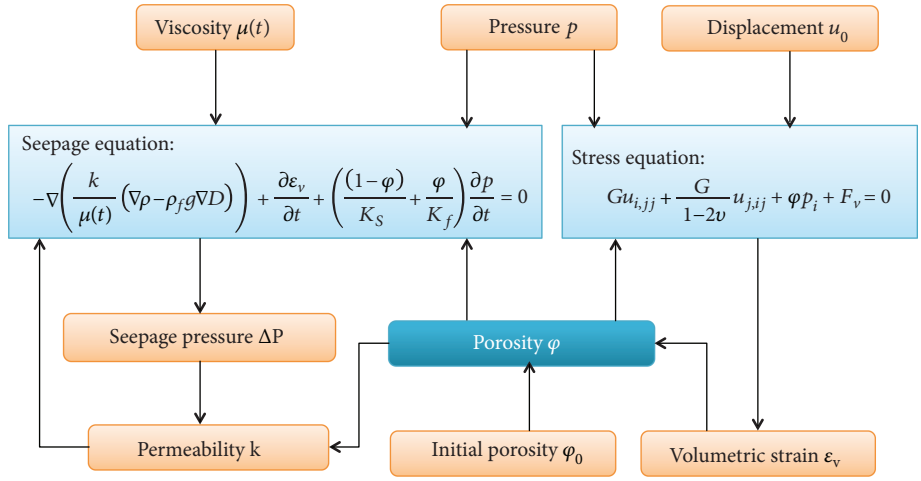

Figure 11: Schematic of numerical analysis.

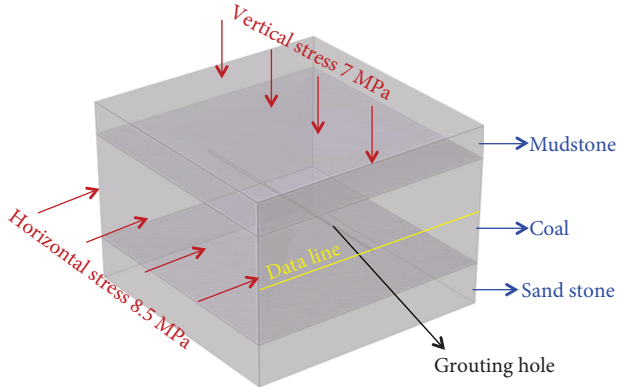

Figure 12: Calculation model.

4.3. Calculation Model and Parameters

4.3.1. Establishment of the Calculation Model. As shown in Figure 12, a calculation model consisting of the grouting of a mudstone roof ($20\times20\times3$ m), coal seam ($20\times20\times10$ m), and sandstone floor ($20\times20\times4$ m) was established. The borehole was in the center of the coal seam and has a diameter of 0.1 m and a depth of 20 m.

4.3.2. Initial and Boundary Conditions

(1) Initial Conditions. Initial slurry pressure in each stratum was set to be 0 MPa.

(2) Stress and Displacement Boundary Conditions. A crustal stress of 8.5 MPa was imposed on the four sides of the model, a vertical crustal stress of 7 MPa was applied on the top surface, the bottom surface was fixed without displacement, and the gas drainage borehole is a free boundary.

(3) Grouting Boundary Conditions. The surrounding four sides of the model were set as symmetric boundary conditions, with the pressure set as 0 MPa, and the top and bottom of each rock stratum have no flow boundary conditions. The grouting pressure at the borehole was set to be P = 1, 2, 3, 4, and 5 MPa.

4.3.3. Model Parameters. The model parameters were obtained from laboratory tests and field tests in Mine 5 of the Yangquan Coal Industry Group, as shown in Table 3.

4.4. Numerical Analysis Results and Discussion. Figure 13 shows the contour and distribution of slurry pressure in the coal seam at 120, 480, and 840 s when the slurry grouting pressure at the borehole is equal to 2 MPa. It can be seen that the pressure of the slurry reaches its maximum at the injection port, which is 2 MPa, and the pressure near the orifice is decaying rapidly, whereas the slurry pressure away from the orifice decreases slowly. As the slurry moves deeper into the coal masses, the pressure gradually decreases and eventually decreases to 0 Pa in the coal seam, which is the maximum diffusion position of the slurry.

Figure 14 shows a comparison of the permeation diffusion range of viscosity time-varying expandable slurry with high water content at a water-cement ratio of 7 : 1 and that of the nonviscosity time-varying slurry whose initial viscosity is the same as that of expandable material with high water content under the same grouting pressure, that is, 2 MPa. It can be seen that the diffusion range of viscosity time-varying expandable materials with high water content is smaller than that of nonviscosity time-varying slurry within the same period of time. As the viscosity of expandable slurry with high water content increases with time, the resistance used by the slurry to overcome the forward movement increases and the permeability diffusion rate of the slurry gradually decreases and the diffusion range of the slurry whose viscosity remains unchanged is greater than that of the slurry whose viscosity keeps increasing within the given time.

Figure 15 shows the pressure distributions of expandable slurries with high water content at water-cement ratios of 6 : 1, 7 : 1, and 8 : 1 at the moment of 480 s under the same grouting pressure, that is, p = 2 MPa. It can be seen that the higher the water-cement ratio, the greater the pressure of

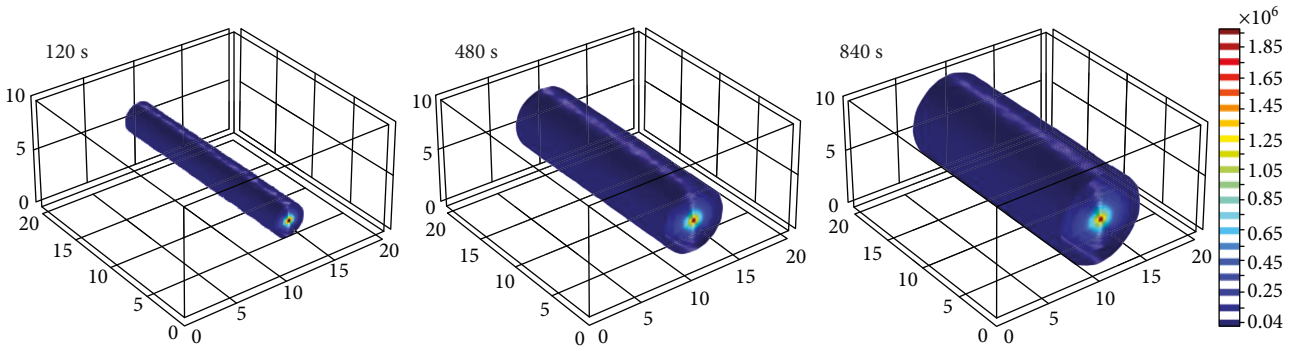

Figure 13: Contour of slurry pressure (grouting pressure $p = 2$ MPa; water-cement ratio of expandable slurry with high water content, W : C = 7 : 1).

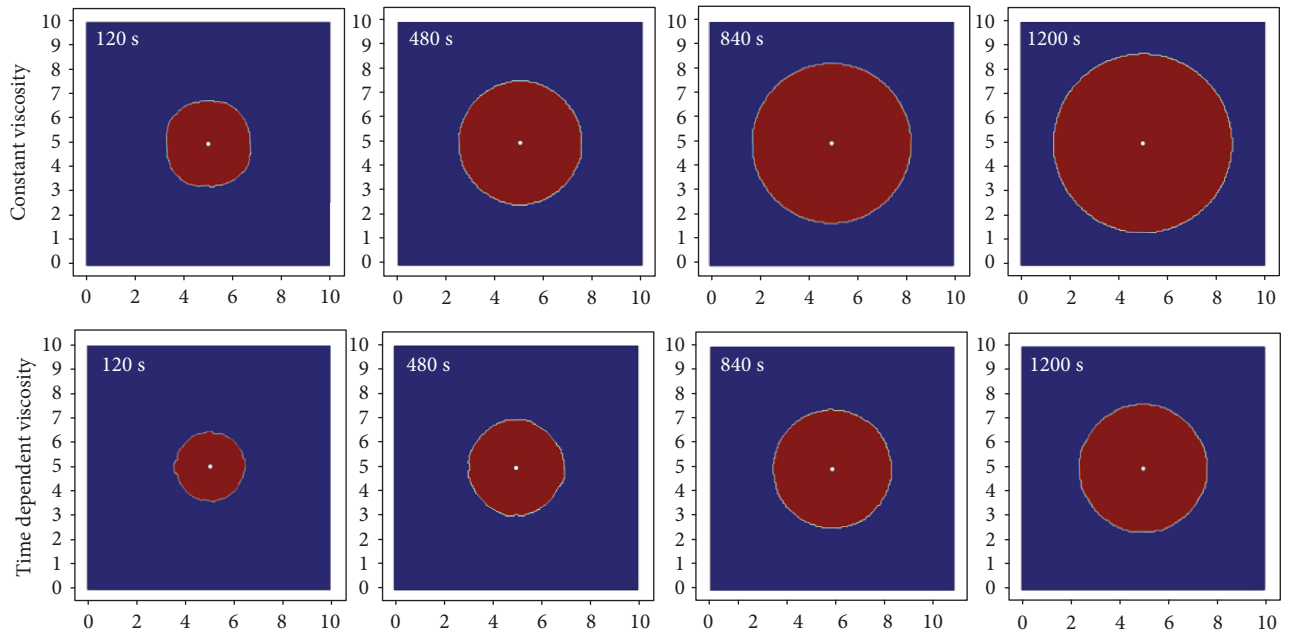

Figure 14: Permeation diffusion range of viscosity time-varying (W : C = 7 : 1, $p = 2$ MPa) and nonviscosity time-varying (0.3 Pa·s, $p = 2$ MPa) expandable slurries with high water content.

the slurry at the same position in the coal seam, indicating that the greater the water-cement ratio, the larger the diffusion range of the slurry at the same moment. The water-cement ratio directly determines the viscosity of the slurry and it is known from the experiment that the higher the water-cement ratio of the slurry, the smaller the viscosity of the slurry. According to the Newtonian viscosity formula [24], the shear stress of the slurry is proportional to its viscosity during the motion. Therefore, the slurry with a small viscosity is affected by less resistance during the movement process, which means that the slurry with a high water-cement ratio tends to have a relatively large diffusion range. Nevertheless, as the water-cement ratio increases, the increase in pressure drops. In addition, according to the experiment, as the water-cement ratio increases, the consolidation strength between the slurry and the coal masses decreases, so the optimal water-cement ratio for grouting is 7 : 1.

Figure 16 shows the pressure distribution of the expandable slurry with high water content at a water-cement ratio of 7 : 1 in the coal seam at the moment of 480 s under different grouting pressures. As the grouting pressure decreases, the slurry pressure in the same position of the coal seam decreases and the decay rate declines as well. When the grouting pressure reaches above 3 MPa, there is little change in the slurry pressure in the same position of the coal seam.

Figure 17 shows the variation of porosity and permeability of the coal masses after being grouted with expandable material with high water content. As indicated by (4) and (5), both the porosity and permeability of the slurry are affected by the grouting pressure P and its volumetric strain ε_v. As shown in the figure, the porosity and permeability share the same variation pattern at the same time. Since the grouting pressure is used to overcome the resistance encountered by the slurry to permeate and diffuse into fractures in the coal seam, the

Table 3: Parameters of different slurries and the strata.

Name	Physical properties		Expression	Units
Viscosity time-varying expandable slurry with high water content	Slurry (W : C = 6 : 1)	Viscosity $\mu_1(t)$	(1)	Pa·s
	Slurry (W : C = 7 : 1)	Viscosity $\mu_2(t)$	(2)	Pa·s
	Slurry (W : C = 8 : 1)	Viscosity $\mu_3(t)$	(3)	Pa·s
	Volumetric compression modulus K_f		1.2×10^{-10}	Dimensionless
Nonviscosity time-varying expandable slurry with high water content	Slurry (W : C = 7 : 1)	Viscosity μ_0	0.3	Pa·s
	Volumetric compression modulus K_f		1.2×10^{-10}	Dimensionless
Coalbed	Initial porosity φ_0		0.38	Dimensionless
	Initial permeability k		8.89×10^{-13}	Dimensionless
	Elastic modulus E		1.85×10^9	Pa
	Poisson's ratio ν		0.31	Dimensionless
	Volumetric compression modulus K_S		1.66×10^9	Pa
Mudstone	Initial porosity φ_0		0.29	Dimensionless
	Initial permeability k		3.48×10^{-14}	Dimensionless
	Elastic modulus E		5.46×10^9	Pa
	Poisson's ratio ν		0.35	Dimensionless
	Volumetric compression modulus K_S		5.45×10^8	Dimensionless
Fine sandstone	Initial porosity φ_0		0.54	Dimensionless
	Initial permeability k		5.17×10^{-10}	Dimensionless
	Elastic modulus E		2.93×10^{10}	Pa
	Poisson's ratio ν		0.23	Dimensionless
	Volumetric compression modulus K_S		5.27×10^{10}	Pa

volume of the coal seam increases near the orifice and the porosity and permeability increase as well. The slurry pressure declines as the slurry flows away from the grouting orifice, and the porosity and permeability decrease with the decline of the grouting pressure, with the initial porosity eventually decreasing to 0.38 and the initial permeability dropping to 8.89×10^{-13}.

Figure 18 shows the diffusion radius of the slurry at a water-cement ratio of 7 : 1 under different grouting pressures. Given the same grouting pressure, the higher the viscosity of the slurry, the larger the diffusion radius of the slurry. Moreover, it can be seen from the figure that once the grouting pressure increases to 3 MPa, the diffusion radius of the slurry will only increase slightly if the grouting pressure further goes up. From the perspective of performance requirements and energy consumption of the grouting equipment, the optimal grouting pressure should be 2-3 MPa, which not only ensures a relatively large diffusion range of the slurry but also saves energy as well as has comparatively low requirements on the grouting equipment.

5. Potential Application for the Mining Industry

In this study, the expandable material slurry with high water content is mainly used for plugging the fractures of coal and rock mass around the gas drainage hole. Its application in plugging the gas drainage hole is reflected in the following aspects: (1) to fill the fractures around the gas drainage hole and seal the air leakage channel, (2) to decrease the permeability of coal and rock around the gas drainage borehole and reduce the amount of air entering the gas drainage hole, (3) to improve the strength of coal and rock mass around the borehole, and (4) to increase the radial support force to the wall of the borehole for resisting the deformation of the borehole and reducing the crack regeneration under the ground stress. Based on the above characteristics, the expandable material slurry with high water content can also be applied to filling the gob, packing roadside along the gob-side entry, and sealing the fractures which water gushes from in the coal mine.

6. Conclusions

(1) According to the experiment results on the setting time of the expandable material with high water content, the setting time of the expandable material with high water content increases as the water-cement ratio increases. The initial settling times of expandable slurries with high water content at different water-cement ratios (4 : 1, 5 : 1, 6 : 1, and 7 : 1) are 15.5, 19, 23, and 25.5 min, respectively, and the final settling times are 148, 172, 205, and 245 min, respectively. It is thus clear that the expandable slurry with high water content is featured by early strength, so it

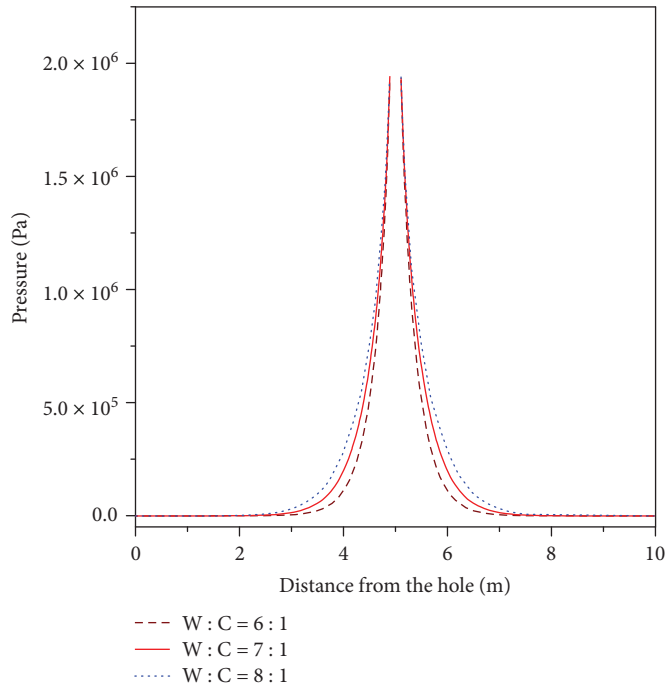

Figure 15: Influences of water-cement ratio on distribution of slurry pressure (time = 480 s, p = 2 MPa).

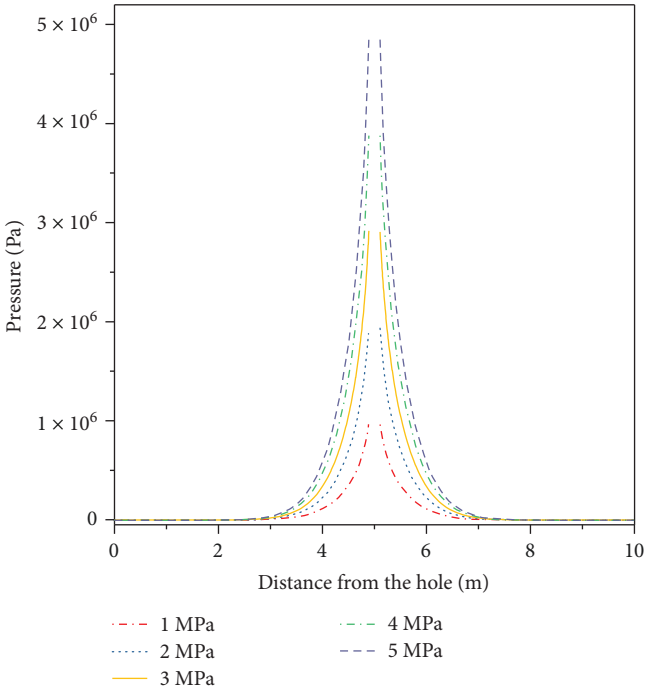

Figure 16: Variation of slurry pressure under different grouting pressures (W : C = 7 : 1, time = 480 s).

can quickly increase the strength of coal and rock masses around the borehole.

(2) The results of the experiment on the viscosity of the expandable material with high water content show that the set-retarding dispersant has little effect on the viscosity of the expandable slurry with high water content and the quick-setting agent and expander C have a relatively large influence on the viscosity of the expandable slurry with high water content, whereas the water-cement ratio has the most significant impact on viscosity of the slurry and such impact phasic. The funnel viscosity of the expandable slurry with high water content increases as the water-cement ratio decreases. The stable slurry with a water-cement ratio above 6 : 1 has great or relatively good groutability, while the slurry with a water-cement ratio less than 6 : 1 features changeable fluidity, poor groutability, or even nongroutability.

(3) As revealed by the results of the experiment on the compressive strength of the expandable material with high water content, the compressive strengths of the expandable material with high water content at water-cement ratios of 9 : 1, 8 : 1, and 7 : 1 decrease as the water-cement ratio increases and their compression resistances are 2.15, 3.42, and 4.26 MPa, respectively. The maximum strengths of compressive failure of expandable slurries with high water content consolidated with coal masses at coal-slurry mass ratios of 9 : 1, 8 : 1, and 7 : 1 is 2.75, 2.23, and 1.28 MPa, respectively. In addition, the smaller the mass ratio and the larger the deformation slope before the peak, the more slurry is grouted into fractures in the coal masses, the greater the elasticity modulus of expandable slurries with high water content consolidated with coal

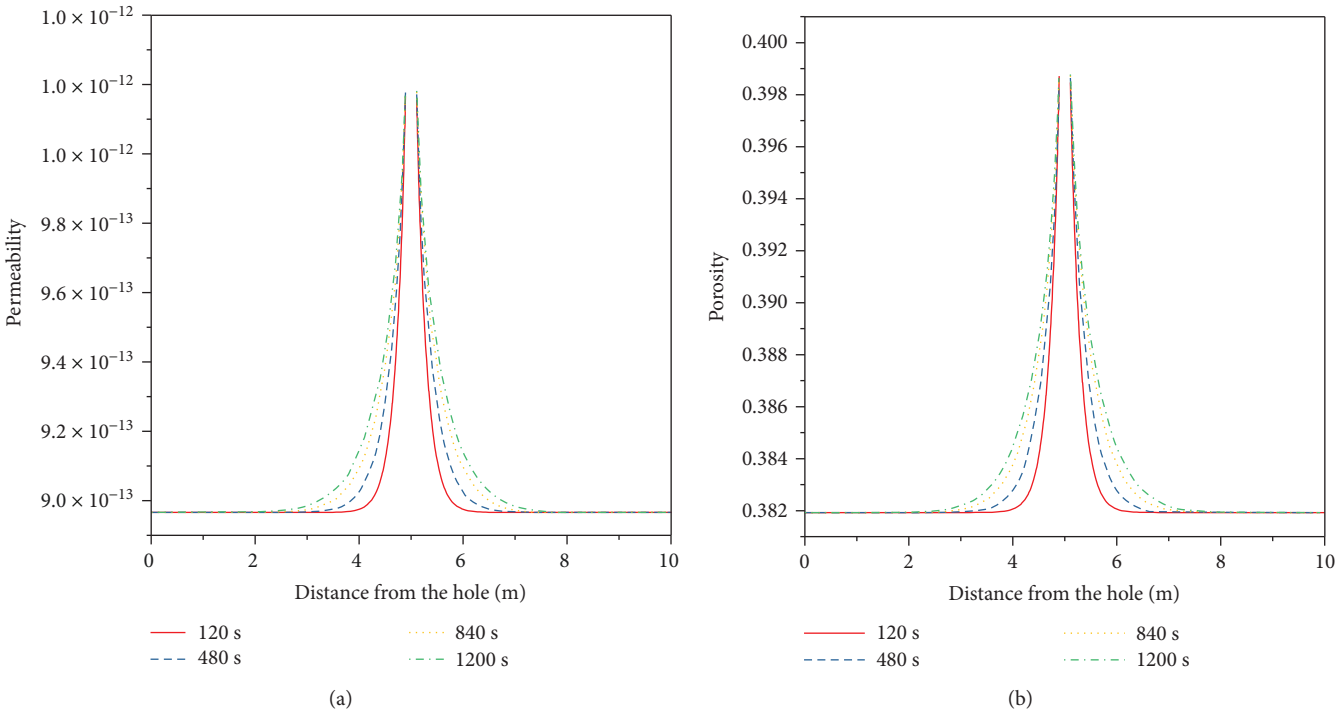

Figure 17: Variation of permeability and porosity over time (W : C = 7 : 1, p = 2 MPa): (a) porosity and (b) permeability.

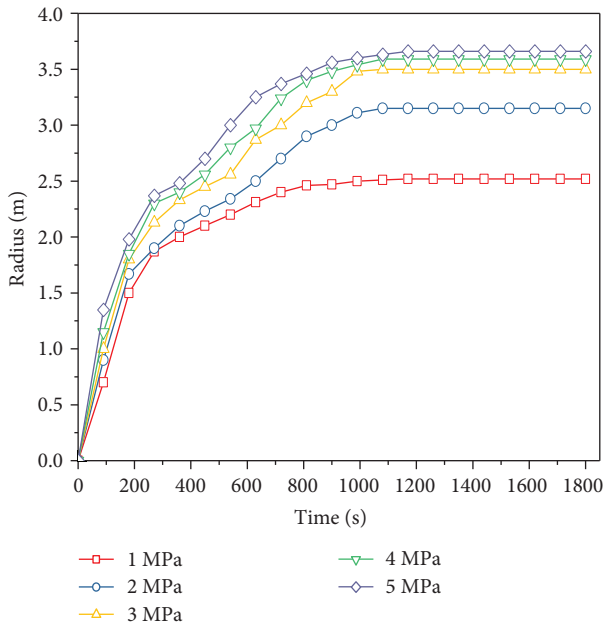

Figure 18: Slurry diffusion radius under different grouting pressures (W : C = 7 : 1).

masses, and the stronger the resistance to deformation and compression failure.

(4) From the permeability experiment and electron microscopic observation, the expandable material with high water content is characterized by low permeability and can be tightly bound to the coal masses, so the expandable material with high water content features low gas permeability after sealing the gas drainage boreholes, which contributes to improving efficiency as well as the concentration of gas drainage.

(5) According to the analysis of the variation pattern of permeability and diffusion of the expandable material with high water content, 2-3 MPa is the optimal grouting pressure that not only ensures a relatively large diffusion range of the slurry but also reduces energy consumption. The higher the water-cement ratio, the larger the diffusion range of the slurry, yet the growth rate of the diffusion range is relatively small, so 7 : 1 is the optimal water-cement ratio that simultaneously satisfies the sealing range and strength. The viscosity of viscosity time-varying expandable material with high water content increases over time, and its diffusion range is smaller than that of nonviscosity time-varying slurry with the same viscosity. The porosity and permeability of strata have a great influence on permeability and diffusion of the slurry, that is, the greater the permeability and the porosity, the larger the permeability and diffusion range of the slurry.

Data Availability

The data used to support the findings of this study are available from the corresponding author upon request.

Conflicts of Interest

The authors declare that they have no conflicts of interest.

Acknowledgments

This work was supported by the National Natural Science Foundation of China (Grant no. 51774279), the Petrochemical Joint Funds of National Natural Science Foundation of China and China National Petroleum Corporation (Grant no. U1762105), and the Fundamental Research Funds for the Central Universities (Grant no. 2015XKZD04).

References

[1] F. Fu, H. Liu, K. R. Polenske, and Z. Li, "Measuring the energy consumption of China's domestic investment from 1992 to 2007," *Applied Energy*, vol. 102, pp. 1267–1274, 2013.

[2] K. Wang, Y. M. Wei, and X. Zhang, "Energy and emissions efficiency patterns of Chinese regions: a multi-directional efficiency analysis," *Applied Energy*, vol. 104, pp. 105–116, 2013.

[3] Y.-P. Cheng, L. Wang, and X.-L. Zhang, "Environmental impact of coal mine methane emissions and responding strategies in China," *International Journal of Greenhouse Gas Control*, vol. 5, no. 1, pp. 157–166, 2011.

[4] F. B. Zhou, J. H. Li, X. Ze, Y. K. Liu, R. G. Zhang, and S. J. Shen, "A study of the second hole sealing method to improve gas drainage in coal seams," *Journal of China University of Mining and Technology*, vol. 38, pp. 764–768, 2009.

[5] Z. F. Wang, U. Zhou, Y. N. Sun, and Y. L. Wang, "Novel gas extraction borehole grouting sealing method and sealing mechanism," *Journal of China Coal Society*, vol. 40, pp. 588–595, 2015.

[6] R. F. Huang, Z. G. Zhang, and B. Cheng, "Study on control mechanism and method of gas concentration in gas drainage borehole of underground mine," *Coal Science and Technology*, vol. 45, pp. 128–135, 2017.

[7] G. Hu, H. Wang, X. Fan, Z. Yuan, and S. Hong, "Mathematical model of coalbed gas flow with Klinkenberg effects in multiphysical fields and its analytic solution," *Transport in Porous Media*, vol. 76, no. 3, pp. 407–420, 2009.

[8] G. Hu, J. Xu, T. Ren, C. Gu, W. Qin, and Z. Wang, "Adjacent seam pressure-relief gas drainage technique based on ground movement for initial mining phase of longwall face," *International Journal of Rock Mechanics and Mining Sciences*, vol. 77, pp. 237–245, 2015.

[9] H. Guozhong, H. Xing, X. Jialin, Q. Wei, and W. Hongtu, "A co-extraction technology of coal and CBM based on the law of gas advanced relieving pressure of in-seam coalface," *Disaster Advances*, vol. 5, pp. 867–872, 2012.

[10] H. U. Guozhong, X. Huang, and X. U. Jialin, "Effect of microwave field on pore structure and absorption of methane in coal," *Journal of China Coal Society*, vol. 40, Supplement 2, pp. 374–379, 2015.

[11] X. Chen, Y. Zhang, W. Sun, X. Ge, and R. Zhao, "Research on expansion property of inorganic hole sealing material of coal mine," *Materials Research Innovations*, vol. 19, no. sup8, pp. S8-142–S8-144, 2015.

[12] Z. F. Wang and W. Wu, "Analysis on major borehole sealing methods of mine gas drainage boreholes," *Coal Science & Technology*, vol. 42, 2014.

[13] Z. X. Hu, "Study of sealing technology of downward & permeable borehole," *Advanced Materials Research*, vol. 524-527, pp. 351–354, 2012.

[14] Q. Ye, Z. Z. Jia, Y. Pi, and H. Z. Wang, "Analysis on sealing method and sealing materials of gas drainage borehole," *Advanced Materials Research*, vol. 716, pp. 485–489, 2013.

[15] B. Flitney, "Positive lubrication rotary seals for down-hole/abrasive applications," *Sealing Technology*, vol. 2005, no. 10, pp. 8–11, 2005.

[16] K. Zhang, K. Sun, B. Yu, and R. P. Gamage, "Determination of sealing depth of in-seam boreholes for seam gas drainage based on drilling process of a drifter," *Engineering Geology*, vol. 210, pp. 115–123, 2016.

[17] C. Zhai, X. Xiang, Q. Zou, X. Yu, and Y. Xu, "Influence factors analysis of a flexible gel sealing material for coal-bed methane drainage boreholes," *Environmental Earth Sciences*, vol. 75, no. 5, p. 385, 2016.

[18] X. Xiang, C. Zhai, Y. Xu, X. Yu, and J. Xu, "A flexible gel sealing material and a novel active sealing method for coal-bed methane drainage boreholes," *Journal of Natural Gas Science and Engineering*, vol. 26, pp. 1187–1199, 2015.

[19] Q. Zou, B. Lin, C. Zheng et al., "Novel integrated techniques of drilling–slotting–separation-sealing for enhanced coal bed methane recovery in underground coal mines," *Journal of Natural Gas Science and Engineering*, vol. 26, pp. 960–973, 2015.

[20] H. Zhou, H. Dai, and C. Ge, "Quality and quantity of predrainage methane and responding strategies in Chinese outburst coal mines," *Arabian Journal of Geosciences*, vol. 9, no. 6, p. 445, 2016.

[21] Y. Ding, G. M. Feng, and C. Z. Wang, "Experimental research on basic properties of superhigh-water packing material," *Journal of China Coal Society*, vol. 36, pp. 1088–1092, 2011.

[22] G. M. Feng, *Research on the Super-High Water Packing Material and Filling Mining Technology and Their Application, [Ph.D. Thesis]*, China University of Mining and Technology, Xuzhou, China, 2009.

[23] GB/T1346-2001, *Test methods for water requirement of normal consistency, setting time and soundness of the Portland cements, China national standard*, State Administration for Market Regulation of the People's Republic of China, 2001.

[24] Y. J. Zhang, *Fluids Mechanics*, Bei-Hang University press, Beijing, China, 1991.

[25] M. J. Pitt, "Martensitic funnel and viscosity of drilling fluid: new equation for oil field application," *Drilling and Completion*, vol. 17, pp. 28–31, 2000.

[26] M. A. Biot and D. G. Willis, "The elastic coefficients of the theory of consolidation," *ASME Journal of Application Mechanic*, vol. 24, pp. 594–601, 1957.

[27] P. C. Li, X. Y. Kong, and D. T. Lu, "Mathematical modeling of flow in saturated porous media on account of fluid-structure coupling effect," *Journal of Hydrodynamics*, vol. 18, no. 4, pp. 419–426, 2003.